

## The Fracture of Nanosilica and Rubber Toughened Epoxy Fibre Composites

By  
A.J. Kinloch, K. Masania and A.C. Taylor,  
*Imperial College London, UK*  
S. Sprenger,  
*Nanoresins AG, Geesthacht, Germany*

### Abstract

The present work describes results obtained for fracture and impact tests for a glass-fibre reinforced modified epoxy composite. Epoxy modification has been achieved by addition of a 1.5 $\mu$ m rubber phase of carboxyl terminated butadiene acrylonitrile (CTBN) and nanosilica (silica particles of the order 20nm diameter) to anhydride cured di-glycidyl ether of bisphenol A (DGEBA) epoxy. Specimens have been produced by resin infusion under flexible tooling. Results show good transfer of toughness from the bulk properties of the modified epoxy. A synergistic effect has also been observed between the nanosilica and rubber, resulting in 50% increase in fracture energy when compared to the rubber modified epoxy. Impact results show that there is a significant rate effect on nanosilica modified composites; with increase in stiffness and much larger delamination in comparison to the other formulations examined. This is a useful property for energy absorption under high strain rate impact.

### Introduction

Epoxyes are favourable as matrices in fibre reinforced composites due to their high crosslink densities. This results in good thermal stability and creep resistance. However, this also results in the composite being brittle and having a poor resistance to fracture and delamination.

It has been found that the addition of rubber particles increases the fracture toughness, but at the cost of decreasing the stiffness of the material, shown by Kinloch [1]. A successful route to counteract this has been to add rigid particles such as nanosilica to the epoxy and rubber blend [2].

A synergistic effect has been observed in nanosilica and rubber toughened epoxyes, with significant increases in toughness without any observable change in the glass transition temperature ( $T_g$ ) or loss of stiffness. The use of a soluble rubber addition and 20nm silica particles are well suited to low cost composite manufacture such as resin infusion under flexible tooling and

vacuum assisted resin transfer moulding as the particles are not filtered out by the fibres during infusion. Previous work has shown that fibre composites have been successfully manufactured with increase in toughness, [3, 4].

In the present work, results from mode I, Charpy and impact tests are reported. Evidence of toughening will be presented with an explanation of mechanisms.

### Materials

The epoxy resin used in this work is a DGEBA, LY556 (Huntsman). This was cured with an accelerated methylhexahydrophthalic acid anhydride: 'Albidur HE 600' (Nanoresins) which was mixed to a stoichiometric ratio.

An organosilane-modified nanosilica, 'Nanopox F400' (Nanoresins) was obtained in a 40wt% DGEBA. They have an average particle size of about 20nm [2].

The rubber was a carboxylterminated butadiene-acrylonitrile (CTBN) rubber, 'Hypro CTBN 1300x8' (Emerald Performance Materials) which has been pre-reacted with DGEBA resin to give a 40wt% CTBN-epoxy adduct, 'Albipox 1000' (Nanoresins).

The formulations were prepared by mixing together the components, to give the required levels of nanoparticles and rubber. Four formulations were used – unmodified epoxy (Control), epoxy with 10wt% silica nanoparticles (Nanosilica), epoxy with 9wt% CTBN (CTBN) and epoxy with 9wt% CTBN & 10wt% silica nanoparticles (Hybrid). Each formulation refers to the percentage of weight of the modifier.

Glass fibre reinforced polymer (GFRP) composite plates were manufactured by resin infusion under flexible tooling. Two fabrics have been used to produce different composite plates. Quasi-isotropic plates were manufactured using a biaxial stitched non-crimp fabric 'XE450/1200' (SP Systems). Composite plates approximately 4mm thick were prepared using 8 plies, laid up in a balanced lay-up to give a 0°/0° interface. Secondly, unidirectional specimens were produced using 'UTE-500' (SP Systems). A 12.5 $\mu$ m thick Poly(tetrafluoroethylene) (PTFE) film was inserted into the fabric prior to resin infusion to act as a starter crack for the fracture specimens. The degassed resin was drawn through the fibres at 50°C, using a vacuum to achieve a near void-free composite. The plates were cured for 2 hours at 100°C, with a post-cure of 10 hours at 150°C. Bulk plates were also manufactured under the same cure conditions.

## Methods

$T_g$  has been measured using differential scanning calorimetry (DSC). 25mg samples of each formulation were heated through two cycles of the range 20°C - 180°C at 10°C/min.  $T_g$  was measured as the point of inflexion for an energy input versus temperature curve.

Flexural modulus tests were conducted on the glass fibre reinforced polymer (GFRP) beams to verify consistency in samples. Tests were conducted on unidirectional GFRP. Flexural modulus was measured using three point bending tests in accordance to ASTM D790M [5].

Single edge notch bend (SENB) tests were conducted on bulk polymer samples to obtain values for initiation fracture energy,  $G_C$  and fracture toughness,  $K_{IC}$ . Tests were conducted in accordance to ISO 13586 [6] and ASTM D5045-91a [7].

Composite mode I fracture energy,  $G_{IC}$  was measured using the Double Cantilever Beam (DCB) test. The fracture energy was calculated using the 'corrected beam theory' method [8-10], Mode II fracture energy,  $G_{IIC}$  was obtained using the End Loaded Split test (ELS) [11]. Results were analysed using the Corrected Beam Theory with Effective crack length method [12]. Tests were conducted on quasi-isotropic beams to avoid significant amounts of fibre bridging during mode I fracture tests.

Short Beam Shear (SBS) tests, [13] have been conducted on unidirectional GFRP to produce a static comparison for the results obtained from the Charpy impact tests. Results are also used to evaluate the fibre matrix interface with varying matrix modification for the systems that are compared. The short beam shear strength was calculated in accordance to ASTM D2344.

Charpy Tests were conducted on short unidirectional GFRP beams at a constant impactor velocity of 1m/s using a servo-hydraulic universal testing machine. The specimen was 50mm in the axial direction (0° fibre orientation) and 20mm width. The span was set to 40mm with a span to thickness ratio of about 10 to generate a large shear force through the specimen upon bending. The specimen was positioned on 8mm diameter pins with the impactor radius controlled to conform to ASTM D6110 [14]. The load was obtained using a 11.2kN piezoelectric loadcell. Displacement was measured using a linear variable differential transducer (LVDT) and was confirmed with the use of high speed photography, see Figure 1. Specimens were un-notched due to a composites' insensitivity to notching under Charpy impact [15].

Ballistic impact was conducted using a gas gun charged with Helium gas. Impact tests were conducted on quasi-isotropic GFRP plates that were 150mm by 100mm by about 4mm thick. The cylinder pressure was varied to obtain different projectile velocities using an 8mm steel ball bearing as the projectile.

## Results

DSC results show that the  $T_g$  changes very little in the composite. At 133±4°C, the addition of nanosilica and CTBN rubber have very little affect to the overall glass transition temperature, Figure 2. These values agree well to bulk tests. This suggests that there is no change in the crosslink density of the epoxy for the different formulations.

Optical microscopy has been conducted on polished cross sections of the composite. These have been used to confirm that the composite is well consolidated and free of voids. The composites have a typical fibre volume fraction of about 57%.

Flexural modulus measurements in Figure 2 show that there is little effect on the composite flexural modulus with change in matrix formulation. This is to be expected with such a highly fibre dominant property. The average flexural modulus is approximately 40GPa.

Atomic force microscopy (AFM) and transmission electron microscopy (TEM) for the bulk has shown that the nanosilica is well dispersed in the epoxy [2]. The same morphology can be found in the fibre inter-space of the composite, suggesting that the fibres do not filter out the nanoparticles, see Figure 3. This has also been verified with scanning electron microscopy (SEM). The CTBN rubber undergoes reaction induced phase separation upon curing. AFM has shown that the typical particle size of rubber is about 1µm. When the Hybrid formulation is cured, the nanosilica in the mix is mobilized; resulting in small clusters of nanoparticles which themselves are well dispersed in the matrix. CTBN rubber particle size increases slightly to 1.5µm, [16].

Bulk fracture tests show (Figure 4) there is little effect on the toughness with the addition of nanosilica. It can be seen that there is a large increase in toughness, about 4 times larger with the addition of CTBN rubber. There is a significant synergy between the nanosilica and rubber particles with a total increase of 6.5 times compared to the unmodified bulk epoxy and 50% larger than the rubber only epoxy. The increase observed in the rubber only epoxy can be explained as enhanced deformation of the epoxy due to interactions between rubber particles and the epoxy ahead of the crack tip, [17, 18]. The further increase of toughness in the hybrid has been postulated as

plastic void formation around the nanoparticles during fracture. This increase in toughness is not observed in the nanosilica only samples as there is no relaxation of the crack tip constraint due to the lack of rubber particles; therefore no further matrix deformation and void growth around particles.

As shown in Figure 4, there is a degree of transfer of toughness from bulk properties to the fibre composite. Results show that there is no difference with the addition of nanosilica only. There is a 75% increase in fracture energy with the addition of CTBN rubber. A 100% increase in the hybrid has been observed although the experimental error is large.

The same large gains in fracture toughness from the bulk have not been fully transferred to the composite. This agrees well with work by Compston et al. [19]. The effect of toughening is decreased due to the large crack tip constraint that is applied by having stiff fibres running through the plastic deformation zone.

Results from mode II and short beam shear tests show no difference in mode II fracture toughness with an average value of 2000 J/m<sup>2</sup> and short beam shear strengths of about 60MPa. It is believed that this is a result of the manufacturing process. An advantageous property of infused composites is their increased resistance to impact because plies are intermingled during the vacuum process. In comparison, a prepreg manufactured composite will have distinct interfaces with resin rich matrix zones between plies.

Charpy impact tests have been used to achieve an instrumented test under high rate to evaluate a simple composite interface. Results have been obtained for maximum shear strength; obtained as the shear stress prior to delamination, and the normalised impact energy that was absorbed by the composite, see Figure 5. A dynamic modulus has also been calculated to compare changes in stiffness at higher rate, see Figure 6. Results show that all the modified formulations have absorbed more energy than the control. This property is useful in trying to optimize a composite structure to absorb energy upon impact. The nanosilica composites show significant rate dependence as the dynamic modulus increases, and the maximum shear stress is largest in this formulation. The inclusion of CTBN rubber gives little increase in maximum shear stress and impact energy. However, the composite also show a loss of stiffness at high rates. It is notable that differences, whilst small, have been observed at higher rates when static values have been shown to be the same across the formulations.

Results from impact tests have focused on the maximum delamination area. Whilst high

velocity impact properties are fibre architecture dominant, it was necessary to examine matrix properties at a high rate. Therefore, test speeds were kept in the range 250m/s to 500m/s; well above the ballistic limit. The front face of the composite plate showed little delamination, with fibre fracture focused on the area that had been penetrated. A graph of delamination area versus cylinder pressure, see Figure 7, shows that the addition of nanosilica has a marked effect on the size of delamination from impact damage. The overall toughness of the nanosilica only composite has decreased dramatically resulting in a large delamination area when compared to all other formulations. There is no difference between the other formulations.

## Conclusions

Nanosilica and CTBN particles have been used to form novel hybrid toughened glass fibre composites. Modified fibre composites have been produced without detriment to flexural modulus or the glass transition temperature. It has been shown that the nanoparticles have not been filtered by the fibre inter-space. Results also demonstrate that there is a transfer of toughness to the composite from the increases that have been observed in the bulk. Rate effects with the addition of nanosilica have also been explored, with increase in composite stiffness; leading to significantly more delamination and energy absorption upon impact; making them favourable for use in energy absorbing structures.

## Further Work

Single fibre fragmentation tests will be conducted to further quantify the differences in interfacial adhesion with matrix modification. This is primarily to verify the findings from mode I tests and help isolate whether changes in toughness are due to matrix deformation or differences in the interface.

Notched and plain strain compression tests on bulk specimens will also be conducted. The aim of these tests is to generate large shear bands and deformation zones in the polymer. Examination of this deformation using TEM, SEM and AFM will aid explanation of the toughening mechanisms that have been postulated.

## Acknowledgements

The authors wish to thank the EPSRC for the studentship of K. Masania and acknowledge the general support from the US Army European Research Office and Emerald Performance Materials.

## References

1. Kinloch, A., *Theme Article - Toughening Epoxy Adhesives to Meet Today's Challenges*. Materials Research Society Bulletin, 2003. **28**(6): p. 445-448.
2. Johnsen, B.B., et al., *Toughening mechanisms of nanoparticle-modified epoxy polymers*. Polymer, 2007. **48**(2): p. 530-541.
3. Kinloch, A., et al., *The interlaminar toughness of carbon-fibre reinforced plastic composites using 'hybrid-toughened' matrices*. Journal of Materials Science, 2006. **41**(15): p. 5043-5046.
4. Kinloch, A., et al., *The Fracture of glass-fibre-reinforced epoxy composites using nanoparticle-modified matrices*. journal of Material Science, 2007.
5. ASTM-D790M, *Standard Test Methods for Flexural Properties of Unreinforced and Reinforced Plastics and Electrical Insulating Materials [Metric]*. 1993, ASTM.
6. BS/ISO-13586, *Plastics - Determination of fracture toughness (K<sub>c</sub> and G<sub>c</sub>) - Linear elastic fracture mechanics (LEFM) approach in British Standards*. 2000.
7. ASTM-D5045-91a, *Standard Test Methods for Plain-Strain Fracture Toughness and Strain Energy Release Rate of Plastic Materials*, in ASTM. 1991.
8. Williams, J.G., *Large Displacement and End Block Effects in the DCB Interlaminar Test in Mode I and Mode II*. Journal of Composite Materials, 1987. **21**: p. 330-347.
9. Williams, J.G., *On the calculation of energy release rates for cracked laminates*, in *International Journal of Fracture*. 1988. p. 101-119.
10. Williams, J.G., *End corrections for orthotropic DCB specimens*, in *Composite Science and Technology*. 1989. p. 367-376.
11. Hashemi, S., A.J. Kinloch, and J.G. Williams, *The Analysis of Interlaminar Fracture in Uniaxial Fibre-Polymer Composites*. Proceedings of the Royal Society of London. Series A, Mathematical and Physical Sciences, 1990. **427**(1872): p. 173-199.
12. Blackman, B.R.K., A.J. Brunner, and J.G. Williams, *Mode II fracture testing of composites: a new look at an old problem*. Engineering Fracture Mechanics, 2006. **75**: p. 2443-2455.
13. ASTM-D2344, *Standard Test Method for Short Beam Shear Strength of Polymer Matrix Composite Materials and their Laminates*. 2000: ASTM.
14. ASTM-D6110, *Standard Test Method for Determining the Charpy Impact Resistance of Notched Specimens of Plastics*. 2006.
15. Bader, M.G. and R.M. Ellis, *The effect of notches and specimen geometry on the pendulum impact strength of uniaxial CFRP*. Composites, 1974. **5**(6): p. 253-258.
16. Kinloch, A.J., et al., *Toughness of nanoparticle-modified epoxy and fibre composites*. Proceedings of the 31st Annual Meeting of The Adhesion Society, 2007.
17. Kinloch, A.J., S.J. Shaw, and D.L. Hunston, *Deformation and fracture behaviour of a rubber-toughened epoxy: 2. Failure criteria*. Polymer, 1983. **24**(10): p. 1355-1363.
18. Kinloch, A.J., et al., *Deformation and fracture behaviour of a rubber-toughened epoxy: 1. Microstructure and fracture studies*. Polymer, 1983. **24**(10): p. 1341-1354.
19. Compston, P.P., *The Transfer of Matrix Toughness to Composite Mode I Interlaminar Fracture Toughness in Glass-Fibre/vinyl Ester Composites*. Applied composite materials, 2002. **9**(5): p. 291-314.

## List of Figures

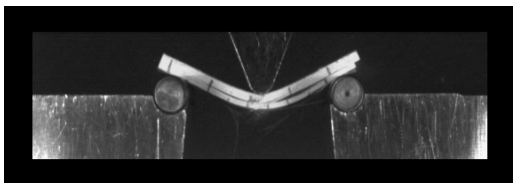


Figure 1: Charpy impact test with a control sample showing considerable interlaminar shear

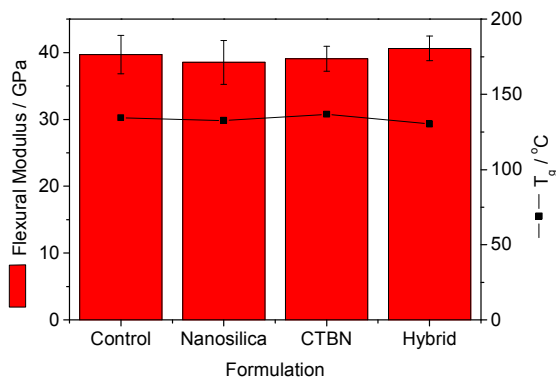


Figure 2: Flexural Modulus and T<sub>g</sub> for the matrix formulations

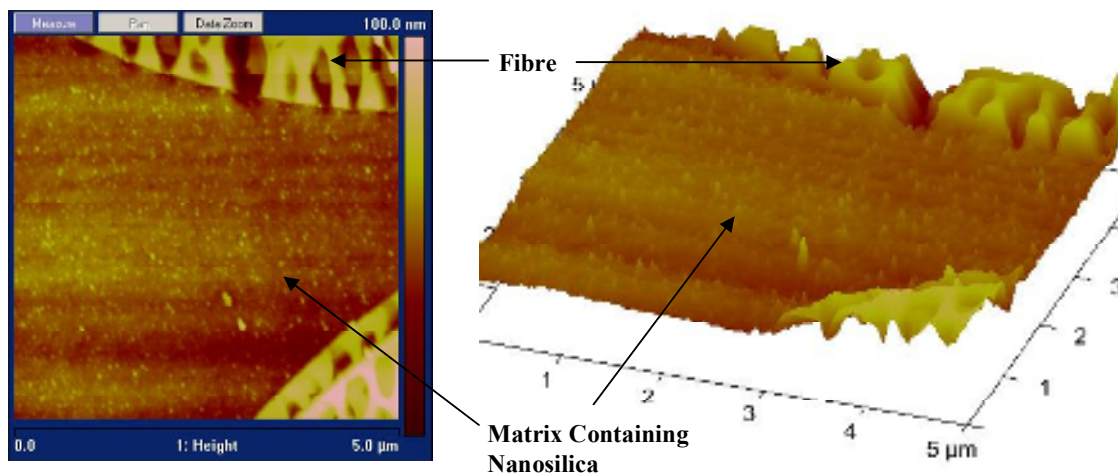
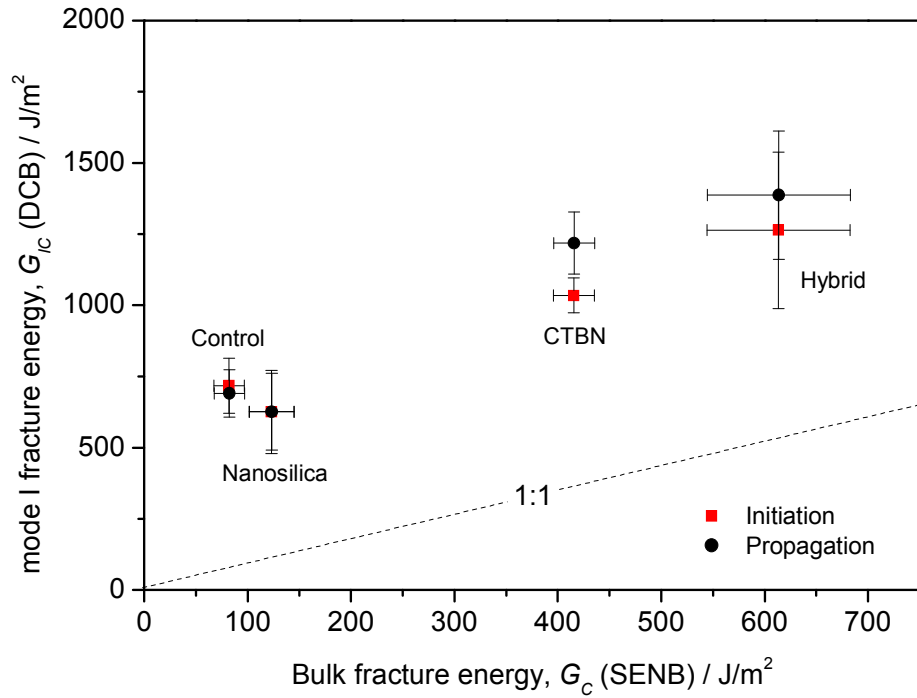
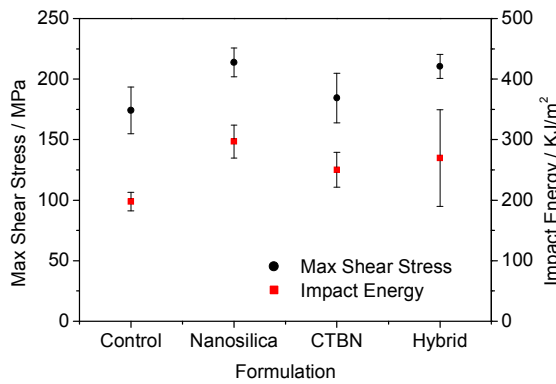


Figure 3: Nanosilica reinforced matrix composite morphology around a glass fibre



**Figure 4: Mode I fracture energy from DCB tests,  $G_{IC}$  vs. Bulk fracture energy,  $G_C$  from SENB tests**



**Figure 5: Maximum shear stress and normalised impact energy for the formulations obtained from Charpy impact tests**

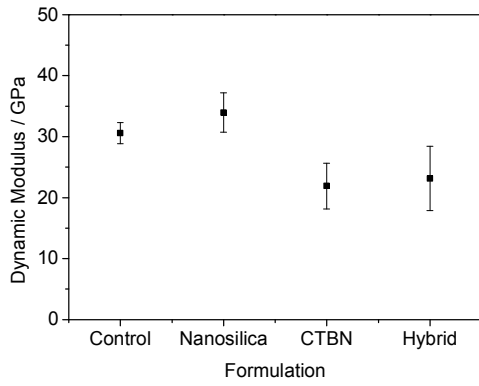


**Figure 6: Dynamic modulus calculated from Charpy impact tests**

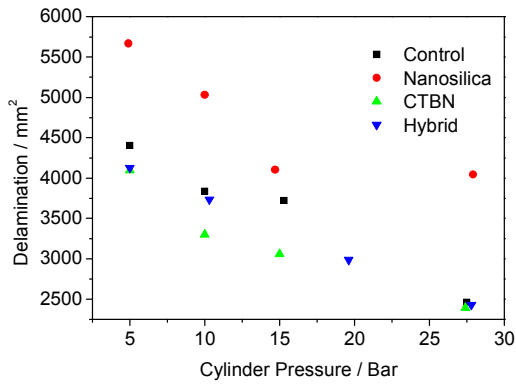


**Figure 7: Delamination area from ballistic impact tests of quasi-isotropic GFRP plates**